Applied Catalysis B: Environmental 241 (2019) 514–520

Contents lists available at ScienceDirect

Applied Catalysis B: Environmental

journal homepage: www.elsevier.com/locate/apcatb

Opposite photocatalytic oxidation behaviors of BiOCl and TiO_2: Direct hole transfer vs. indirect ˙OH oxidation

Junbo Zhong[a,b], Yukun Zhao[a], Liyong Ding[a], Hongwei Ji[a], Wanhong Ma[a], Chuncheng Chen[a,*], Jincai Zhao[a,*]

[a] Key Laboratory of Photochemistry, Beijing National Laboratory for Molecular Sciences, Institute of Chemistry, Chinese Academy of Sciences, Beijing, 100190, PR China
[b] Key Laboratory of Green Catalysis of Higher Education Institutes of Sichuan, College of Chemistry and Environmental Engineering, Sichuan University of Science and Engineering, Zigong, 643000, PR China

ARTICLE INFO

Keywords:
Photocatalytic degradation
Perhalocarboxylate acids
BiOCl
TiO_2
Hole transfer
Water activation

ABSTRACT

Although all the semiconductor-based photocatalysis is initiated by photoinduced conduction band electron and valence band hole, the reaction pathway and activity of the electron and hole would be largely dependent on the type of the photocatalyst. It is essential to distinguish and understand the photocatalyst-dependence of a specific reaction. In the present study, we compared the photocatalytic behaviors of BiOCl and TiO_2 for the degradation of different pollutants including perfluorooctanoic acid (PFOA), chloroacetic acids and benzoic acid. We found that the decompositions of perhalocarboxylate acids (PHCAs) such as PFOA and trichloroacetic acid (TCA) were much rapider over BiOCl than on the TiO_2 (commercial P25). The surface-area- normalized rate constants for the oxidation of TCA have five orders of magnitude of difference between these two systems. By contrast, the degradation rates of ˙OH-sensitive organic pollutants such as dichloroacetic acid, monochloroacetic acid and benzoic acid were much higher on the TiO_2. Moreover, much more meta-substituted hydroxylated intermediate was observed during the photocatalytic oxidation of benzoic acid on BiOCl. In addition, PFOA and TCA were degraded efficiently in the BiOCl system even in the presence of other labile organic compounds (such as acetic acid). All the experimental results definitely indicate that BiOCl photocatalyst prefers to directly oxidize the PHCAs and benzoic acid by the hole transfer, while TiO_2 tends to oxidize the solvent water molecule to ˙OH radical. The mechanism underlying on the different activity of BiOCl and TiO_2 are further discussed.

1. Introduction

Semiconductor-based photocatalysis represents a promising technique to the treatment of waters contaminated with organic compounds. During the past 40 years, various photocatalysts with different components, structures and properties have been developed [1,2]. These photocatalysts are usually reported to exhibit high photo-efficiency by testing the degradation activity of one or several model pollutants. All the photocatalytic reactions share the common initial step-the production of the reductive conduction band electrons (e_{cb}^-) and oxidative valence band holes (h_{vb}^+) by the excitation of the semiconductor photocatalysts. However, the followed reactions of the electron and hole on the surface of photocatalysts can be very different. Depending on the intrinsic surface structure of the photocatalyst, a specific redox reaction has different reaction pathway and activity on different photocatalysts. For the selective degradation of specific pollutant, it is essential to distinguish and understand the dependence between photocatalyst and the type of degradation reaction. However, the photocatalyst-dependence of a specific degradation reaction and the substrate-dependence of a given photocatalysts are less investigated and understood so far. For example, bismuth oxychloride (BiOCl) is a layered ternary oxide semiconductor and has been extensively reported for its photocatalytic activity on the degradation of organic pollutants [3–9]. Most of the reports focus on the synthesis of the BiOCl nanostructures with different morphologies and exposed facets [5,6,8], or on understanding the electronic structures by theoretical calculation [10–14]. Usually, the photocatalytic activity of synthesized BiOCl material is tested by degrading some model pollutants such as dyes [3–5]. Sometimes, the photoactivity of BiOCl is also compared with TiO_2 [4]. The facet-dependent photoreactivity for photodegradation of methyl orange (MO) or molecular oxygen activation has also been investigated [15,16]. However, the difference in photocatalytic behaviors for the degradation of different pollutants between the BiOCl and other photocatalyst such as the most-studied TiO_2 are not systematically

* Corresponding authors.
E-mail addresses: cchen@iccas.ac.cn (C. Chen), jczhao@iccas.ac.cn (J. Zhao).

https://doi.org/10.1016/j.apcatb.2018.09.058
Received 10 May 2018; Received in revised form 14 August 2018; Accepted 17 September 2018
Available online 24 September 2018
0926-3373/ © 2018 Elsevier B.V. All rights reserved.

compared, although the photocatalytic performances have been separately investigated under different reaction conditions. Such a comparison would be helpful to the selection of photocatalyst toward different target pollutants.

Perhalocarboxylate acids (PHCAs) such as perfluorooctanoic acid (PFOA) and trichloroacetic acid (TCA) represent a large kind of the polyhalogenated organic pollutants. These compounds are attracting increasing concerns due to their global occurrence, potential toxicity and high recalcitrance. As the most famous perhalocarboxylate pollutant, PFOAs has been frequently detected in environmental waters, animals, and human tissues all over the world [17,18]. However, the treatment for these pollutants is challenging [19–22]. The electron-withdrawing properties of halogen and the carboxylate group make these pollutants difficult to be oxidized by losing electron (electron transfer pathway). In addition, hydroxyl radical, which is the dominant active species in the advanced oxidation systems, is ineffective for the degradation of PFOA and TCA. Particularly, the most frequently used photocatalyst TiO_2 is reported to be ineffective to decompose PFOA, although the photocatalytic destruction of PFOA can be observed over TiO_2 under strongly acidic aqueous solution [23–26]. However, β-Ga_2O_3 and In_2O_3 were found to possess higher PFOA degradation activities than TiO_2 [27–29]. Very recently, Song et al. also reported that BiOCl is efficient for the photocatalytic decomposition of PFOA [7]. The reason underlying the superior activity of these photocatalysts is not fully understood.

In the present study, being aimed at shedding light on the photocatalyst-dependence of different degradation reaction, we compared systematically the photocatalytic behaviors between the BiOCl and benchmark commercial TiO_2 (Degussa P25) for degradation of PHCAs and other pollutants. Our results indicate that BiOCl is very effective for the degradation of the PHCAs. By contrast, TiO_2 exhibits much higher activity for the degradation of the pollutants such as chloroacetic acid and benzoic acid that are sensitive to the $^{\cdot}OH$ radical. The mechanism on the different photocatalytic behaviors of BiOCl and TiO_2 is further discussed, which would provide helpful insights for the understanding of structure-activity of the photocatalyst and the selectivity removal of organic pollutants. It is of great significance to find that these two photocatalysts exhibit quite different pathway for the oxidative degradation of the organic pollutants, since both the degradation reactions are initiated by the common oxidative species: the valence band hole. By the systematic comparison, in addition, we can get some new understanding on the photocatalytic reaction on both TiO_2 and BiOCl.

2. Experimental section

2.1. Chemicals

Perfluorooctane sulfonate (PFOS), perfluorooctanoic acid (PFOA), and trichloroacetic acid (TCA), dichloroacetic acid (DCA), monochloroacetic acid, acetic acid and $Bi(NO_3)_3{\cdot}5H_2O$ were of analytical grade and used without further purification. Deionized water was used in all the experiments.

2.2. Preparation and characterization of BiOCl photocatalyst

BiOCl was synthesized by a typical hydrothermal synthesis. [8] Briefly, 5 g $Bi(NO_3)_3{\cdot}5H_2O$ was dissolved in 20 mL glacial acetic acid under intense stirring, then KCl aqueous solution (0.769 g KCl + 10 mL H_2O) was added dropwise to the above $Bi(NO_3)_3{\cdot}5H_2O$-acetic acid solution under intense stirring, forming white precipitate. The suspension system was transferred into a 100 mL Teflon-lined stainless-steel autoclave. The autoclave was maintained at 453 K for 24 h and then cooled to room temperature naturally. The resulting white product was collected by filtration, and washed with deionized water and absolute ethanol many times, and then dispersed in absolute ethanol and dried naturally.

Scanning electron microscope (SEM) images were taken with a Hitachis 4880 scanning electron microscope, using an accelerating voltage of 10 kV. The specific surface area (SBET) value was obtained on a QUADRASORB automatic surface analyzer (Quantachrome, America) by the Brunauer-Emmett-Teller (BET) method. Crystalline phases of the prepared photocatalyst was identified by X-ray powder diffraction (XRD) on a X-ray diffractometer a Hitachis 4880 (Panalytical, EMPYR) with Cu Kα radiation. The X-ray tube was operated at 40 kV and 40 mA.

2.3. Photocatalytic decomposition of model pollutants

In a typical photocatalytic experiment, 40 mg the photocatalyst was dispersed in 40 mL model pollutant solution by intense stirring. The photocatalytic reaction was carried out in a 50 mL quartz reactor with a recycling water glass jacket to keep the reaction temperature at 298 K. The light source was a 500 W xenon lamp (simulated sunlight, containing 4% UV light). Prior to irradiation, the suspensions were magnetically stirred in the dark for 1 h to establish an adsorption- desorption equilibrium. At given time intervals, 3 mL of suspension was centrifuged and the upper solution was sampled for analysis.

2.4. Analysis

The concentration of acetic acid, monochloroacetic acid, dichloroacetic acid, trichloroacetic acid and F^- were measured with an ion chromatography (Dionex DX300) equipped with an Ion Pac AS11-HC analytical Column (4 × 250 mm) column and a degasser. The eluate was 15 mM NaOH, the flow rate was 1 mL/min. Analysis of PFOA and the intermediates was accomplished by high performance liquid chromatography (Ultimate 3000 HPLC, Thermo Fisher, USA) equipped with an electrospray ionization tandem mass spectrometer (AB SCIEX Triple quad™ 3200, AB SCIEX, USA) operated in negative mode. The separation was achieved on an Acclaim 120 C_{18} column (5 µm, 4.6 mm i.d. × 150 mm length; Thermo Fisher) after the injection of a 10 µL aliquot of sample. A 10 min dualistic gradient of 0.1% ammonium hydroxide (in methanol) and 50 mM NH_4OAc at a flow rate of 1.0 mL/min was optimized as follows: an initial 28% 50 mM NH_4OAc was reduced to 5% at 4 min before returning to the original condition at 7 min. Quantitative analyses were then conducted using ESI/MS/MS.

3. Results and discussion

3.1. Synthesis and characterization of BiOCl photocatalyst

The BiOCl used in this study was synthesized by a typical hydrothermal method. In agreement with the previous study [8], the obtained BiOCl displays sheet-shaped structures (Fig. S1). The XRD analysis showed that all the diffraction peaks of BiOCl can be indexed to the tetragonal crystal structure, which coincides with the standard JCPDS file of BiOCl (No.06-0249). No other XRD patterns can be observed, indicating high purity of the as-prepared BiOCl sample (Fig. S2).

3.2. Degradation of PFOA on BiOCl and TiO_2

We first compared the photocatalytic defluorination of PFOA in the BiOCl and TiO_2 systems under simulated sunlight irradiation. Fig. 1A shows the time course of release of inorganic fluoride ion during irradiation. As for BiOCl, about 70% of the fluorine atoms, equivalent to about 10 of 15 fluorines in PFOA, were released after irradiation of 12 h. By contrast, less than 5% of the fluorine release was observed under the otherwise identical conditions in TiO_2 system. Similarly, BiOCl also exhibited significant photocatalytic activity for the degradation of another even resistant perfluorinated pollutants perfluorooctane sulfonate (PFOS), for which TiO_2 is completely ineffective (Fig. S2).

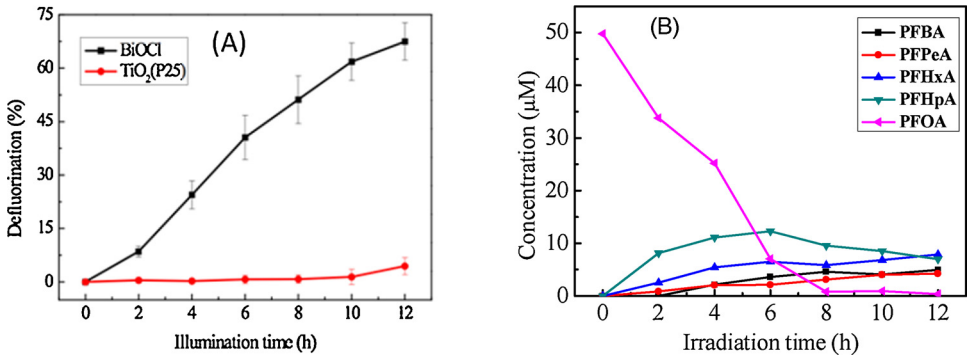

Fig. 1. (A) Release of F^- during photocatalytic degradation of perfluorooctanoic Acid (PFOA) on BiOCl and TiO_2 under simulated sunlight irradiation. (B) The decay of PFOA and formation of perfluorocarboxylate acids (PFCAs) with shorter carbon chain length. Catalyst concentration: 1 g/L; PFOA: 20 mg/L. Each error bar represents the standard deviation from the mean of three experiments.

The degradation of PFOA and formation of intermediates were identified and quantified by HPLC-MS. Besides fluoride ions, the photocatalytic degradation of PFOAs also lead to the formation of perfluorocarboxylate acids (PFCAs) with shorter carbon chain length, such as perfluoroheptanoic acid (PFHpA), perfluorohexanoic acid (PFHxA), perfluoropentanoic acid (PFPeA), perfluorobutanoic acid (PFBA). The PFCAs with carbon chain length of less than 4 were not detectable during the tested time. Actually, no degradation was observed by using trifluoroacetic acid as model PFCAs, indicating that BiOCl is infective for degradation of PFCAs with 2 and 3 carbon chain. Even so, considering that the PFOAs with a longer carbon chain length ($n > 7$) are more bioaccumulative, the toxicity of the degradation products should be much less than the original PFOA. The time profiles for shorter-chain PFCAs intermediates are shown in Fig. 1B. Along with the decrease of the PFOA, the C7 PFCA (PFHpA) was generated rapidly, and reached its maximum concentration at 6 h of irradiation. After that, a gradual decrease in the concentration of PFHpA was observed. Such a time dependence of PFHpA intermediates indicates that the degradation of PFOA proceeds in a stepwise manner from C_n to C_{n-1} PFCAs.

3.3. Degradation of chloroacetic acids on BiOCl and TiO_2

The superior photocatalytic activity of BiOCl, relative to that of TiO_2, was also observed in the degradation of trichloroacetic acid (TCA). As shown in Fig. 2A, the apparent first order rate constant for the degradation of TCA on BiOCl (0.89 h^{-1}) was 400 times than that on TiO_2 (0.0022 h^{-1}). Moreover, considering the surface area of the employed BiOCl (1.87 m^2/g) is much smaller than that of TiO_2 (50 m^2/g) (Table 1), the difference in the surface area normalized rate constant between these systems was even larger, up to five orders of magnitude. In contrast, the degradation of dichloroacetic acid (DCA), in which one of the Cl atoms of TCA is substituted by H, on TiO_2 ($k = 0.40\ min^{-1}$) was much rapider than that on BiOCl ($k = 0.032\ min^{-1}$) (Fig. 2B). Similarly, the degradation of monochloroacetic acid (MCA, Fig. 2C) and acetic acid (AC, Fig. 2D) were also much rapider on TiO_2 than on BiOCl. The inversed relative activity for degradation of TCA and other acetic acids suggests a distinct photocatalytic behavior of the two systems. Similar to PFOA, the full chlorinated TCA is resistant to the attacking of ˙OH radical, and the direct oxidation by hole is the dominant pathway for its photocatalytic oxidative degradation. However, because of the presence of C–H bond, which is susceptive to the attacking of the ˙OH radical, the ˙OH radical can abstract easily the hydrogen atom from DCA, MCA and AC to initiate the oxidation reaction.

3.4. Degradation of benzoic acid on BiOCl and TiO_2

The degradation of benzoic acid (BA) was also investigated on BiOCl and TiO_2 surface. As shown in Fig. 3A, the degradation of BA on TiO_2 ($k = 0.208\ min^{-1}$) was much rapider than that on BiOCl ($k = 0.03\ min^{-1}$). Moreover, a remarkable difference in the distribution of intermediates, which is crucial to the detoxication of pollutants, between these two systems was observed. During the degradation, similar amount of para-substituted hydroxylated benzoic acid was detected the on BiOCl and TiO_2 surface (Fig. S4). However, the accumulation of meta-substituted hydroxylated intermediates in the TiO_2 system was much more significant than that on BiOCl. On TiO_2, the ratio of meta-hydroxyl benzoic acid to the para-hydroxylated one was about 4 at conversion rate of 38% and increased with the further conversion. In contrast, on BiOCl, the ratio was only 2 at the similar conversion and decreased with the irradiation time (Fig. 3B).

The difference in the intermediate distribution again indicates the distinct photocatalytic behavior between BiOCl and TiO_2. One of the pathway for the formation of the hydroxylated products is attacking of BA by ˙OH radical (Pathway A in Scheme 1). The earlier theoretical calculations showed that the rate constants for the reaction of benzoic acid and hydroxyl radicals follow the order of meta addition > para addition > ortho addition [30]. The accumulation of meta-hydroxylated intermediates in the TiO_2 suggests that the attacking of ˙OH radical should be dominant mechanism in this situation. On the other hand, the one-electron oxidation potential of BA (E_{BA}°) is estimate to be 2.6 V vs. NHE [31–33], which is near the oxidation potential of E_{VB} of TiO_2 (~2.7 V vs. NHE) [34], but lower than that of BiOCl (~3.5 V vs. NHE [35]). It is thermodynamically possible that BA can be directly oxidized by valence band hole (Pathway B in Scheme 1). The intermediate distribution initiated by this direct hole oxidation pathway might be different from that by the •OH-attacking mechanism. Therefore, we propose that the BA degradation might occur through the direction hole oxidation on BiOCl.

3.5. Degradation of PHCAs in the presence other organic compounds on BiOCl

In waters, the PHCAs usually co-exist with other OH-sensitive compounds, which would hinder the degradation of PHCAs in the advanced oxidation processes by the competition for the active oxygen species. The superior photocatalytic activity of BiOCl for the degradation of PHCAs over other organic compounds implies that the influence of the co-existed organic compound may be insignificant in the BiOCl system. To test this speculation, we examined the degradation rate of PFOA and TCA when they co-exist with acetic acid in the system. It is observed that, on the BiOCl, the presence of acetic acid only reduced slightly the photocatalytic release of F^- from the PFOA (Fig. 3A), which means that the degradation of the refractory PFOA still occurs smoothly on BiOCl surface, even coexisting with the more labile acetic acid. Interestingly, as shown in Fig. 3B, the presence of acetic acid enhances the degradation of TCA to some extent on the surface of BiOCl, while the degradation of acetic acid is not changed much by the presence of TCA. Different from the PFOA, TCA can be reduced by the conduction band electron or the radicals formed during the photocatalytic oxidation of acetic acid. Therefore, in this system, the two pathways for the decomposition of TCA occur: the oxidation pathway and the reduction pathway. The occurrence of the reduction pathway is verified by the

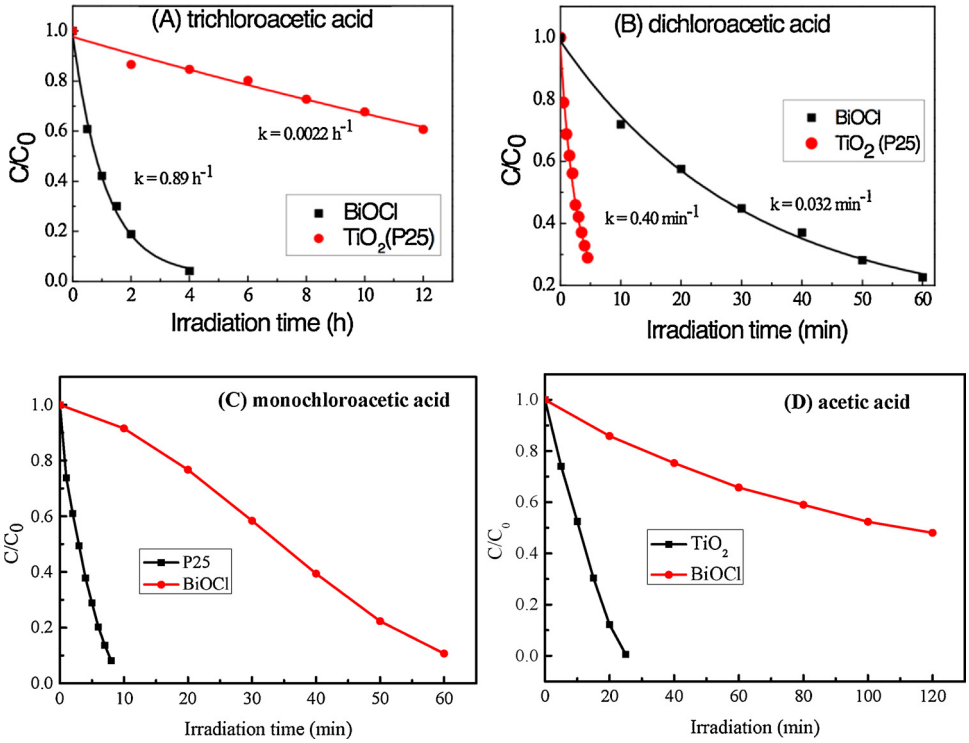

Fig. 2. Photocatalytic decomposition of trichloroacetic acid (A), dichloroacetic acid (B), monochloroacetic acid (C) and acetic acid (D) on BiOCl and TiO_2 surface under simulated sunlight irradiation.

Table 1
Isotherm parameters of trichloroacetate adsorption on different photocatalysts at 298 K.

Catalyst	$S_{BET}(m^2/g)$[a]	q_m (μg/g)[b]	q_m (μg/m^2)[c]	b(L/μg)[d]
BiOCl	1.87	526	281.3	0.38
P25	50	2000	40.0	0.093

[a] The Brunauer-Emmett-Teller (BET) specific surface area (SBET) of BiOCl and TiO_2 (P25) nanocrystals.
[b] The maximum adsorption amount of TCA in the unit of μg/g.
[c] The maximum adsorption amount of TCA in the unit of μg/m^2.
[d] The adsorption equilibrium constant.

formation of dichloroacetic acid in the presence of acetic acid. This can well explain the enhancement for the degradation of TCA in the presence of acetic acid.

4. Discussion

Most of the current reports on the degradation of the PFOAs are based on the oxidative Kolbe-like decarboxylation. For example, the persulfate activated by UV light [36], heat [37], and microwaves [38] are reported to the efficient oxidative degradation of PFOA. Other harsh conditions, such as gamma-irradiation [39], 185 nm vacuum ultraviolet [40,41]. high concentration of H_2O_2 [42]. Electrochemistry [19,22,43] and Sonochemistry [44,45] are also reported to be effective for the degradation. The stepwise decarboxylate of PFOA on BiOCl should be also initiated by direct hole oxidation. During this process, the adsorbed PFOA anion ($CF_3(CF_2)_6COO^-$) donates an electron to the photoinduced hole to generate PFOA radical (Eq. (1)). The cleavage of C—C bond in this high-energy radical (Kolbe decarboxylation reaction) leads to the formation a C7 radical ($CF_3(CF_2)_5CF_2^{\cdot}$) and the release of CO_2 (Eq. (2)).

$$CF_3(CF_2)_6COO^- + h_{vb}^+ \rightarrow CF_3(CF_2)_6COO^{\cdot} \quad (1)$$

$$CF_3(CF_2)_6COO^{\cdot} \rightarrow CF_3(CF_2)_5CF_2^{\cdot} + CO_2 \quad (2)$$

$$CF_3(CF_2)_5CF_2^{\cdot} + O_2 \rightarrow\rightarrow CF_3(CF_2)_5COO^- + 2F^- \quad (3)$$

The C7 radical further undergoes a complex reaction by reacting with molecular oxygen and water, to generate perfluoroheptanoic acid (PFHpA) and F^- (Eq. (3)), during which many unstable intermediates such as peroxoradicals and primary perfluorinated alcohol may be involved, as in the situation of $SO_4^{-\cdot}$-based PFOA oxidation [46].

The present study shows that the BiOCl prefers to directly oxidize the PHCA anion or BA, while the TiO_2 tends to oxidize the water molecule to $^{\cdot}OH$ radical prior to the direct oxidation of the substrate. It is possible that the preferential hole transfer to PHCAs or BA on BiOCl is attributed to the higher oxidation potential of E_{VB} of BiOCl (~3.5 V vs. NHE [35]), compared to that of TiO_2 (~2.7 V vs. NHE). However, if only the potential is considered, both the oxidation of PHCA and water would be more favorable on BiOCl. In addition, the photocatalytic reaction is carried out in the aqueous solution, which means that there is much higher concentration of water molecules (55.6 M) than that of the PHCA (56.1 μM for PFOA). Therefore, only the higher potential cannot explain well the superior activity of BiOCl for oxidation of PHCA.

The pKa value of PFOA,TCA and DCA is 2.8, 0.64 and 1.3, respectively, while the point of zero charge for BiOCl and TiO_2 is pH = 2.8 and pH = 6.4, respectively. At the employed pH ~ 4, both PFOA and TCA are in their ionic form and the surface of the BiOCl and TiO_2 is negatively and positively charged, respectively. Therefore, the electrostatic interaction between the TCA and the photocatalyst surface cannot explain the stronger adsorption of TCA and BiOCl. In addition, the DCA is also in its ionic state (pKa = 1.3). The distinct degradation behavior between TCA and DCA also indicates that the surface charge play a minor role in their different adsorption and degradation behavior on BiOCl and TiO_2.

More reasonably, the specific surface structure of BiOCl and TiO_2 may be dominant in their different photocatalytic behavior. To verify this, we further compared the adsorption behavior of TCA on BiOCl and TiO_2 surface. The adsorption isotherm profiles are shown in Fig. 4A. The adsorption constant can be calculated by Eq. (4):

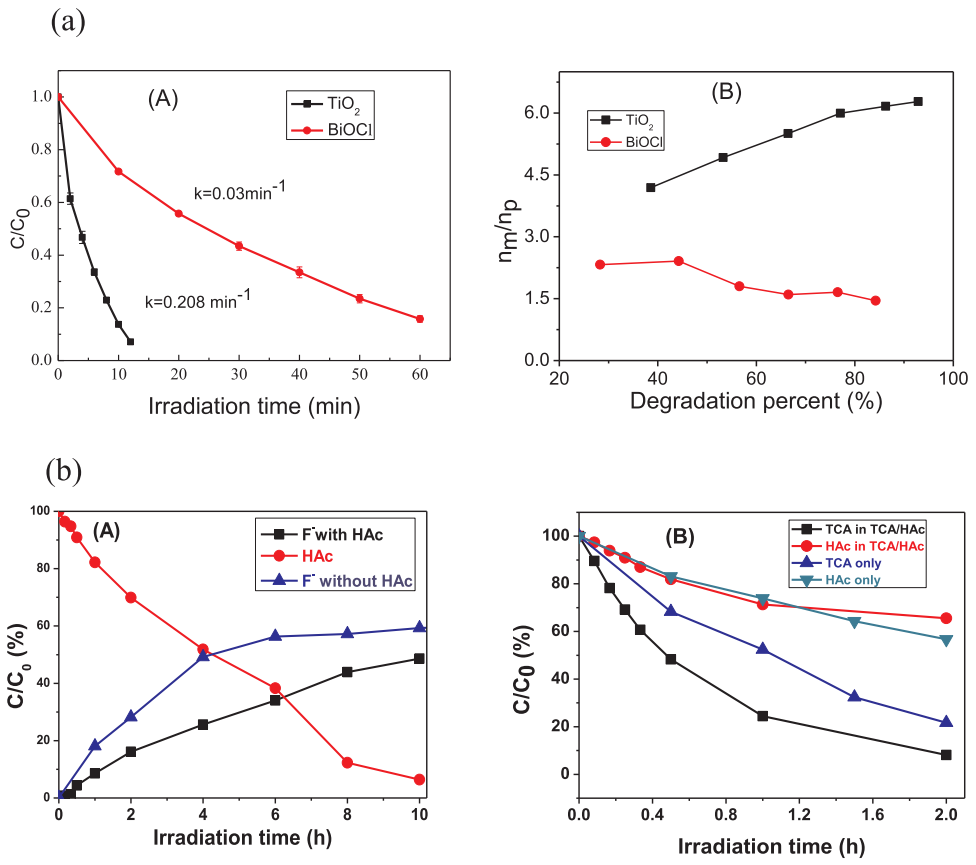

Fig. 3. (A) Photocatalytic decomposition of benzoic acid on BiOCl and TiO_2 surface under simulated sunlight irradiation. (B) The ratios of produced meta-hydroxyl benzoic acid and the para-hydroxylated one on these two photocatalysts. (B) Photocatalytic decomposition of (a) PFOA (20 mg/L) and (b) TCA (20 mg/L) in the presence of acetic acid (20 mg/L) on BiOCl under simulated sunlight irradiation.

$$\frac{p_e}{q_e} = \frac{1}{q_m}p_e + \frac{1}{q_m b} \quad (4)$$

where b is the adsorption equilibrium constant; ρ_e is the equilibrium concentration of the TCA, q_e is the adsorbed TCA on the photocatalysts; and q_m is the maximum adsorption of TCA. Fig. 4B shows the adsorption isotherms with the fittings to Eq. (4) for BiOCl and TiO_2 catalysts, and the fitted adsorption parameters are listed in Table 1. The excellent linear relationships between ρ_e/q_e and ρ_e curves on both photocatalysts confirm that the measured adsorption isotherms agree well with the Langmuir adsorption model. The estimated q_m value for TCA is 546 and 2000 μg/g, respectively, on BiOCl and TiO_2 catalysts (Table 1). Considering that the Q_m is directly proportional to the number of active adsorption sites on the photocatalysts, the maximum adsorption is relevant to the effective surface area. After normalized by surface area, the Q_m on BiOCl surface (281.3 μg/m^2) becomes much larger than that on the surface of TiO_2 (40.0 μg/m^2), which means that much more density of adsorption sites for TCA on BiOCl surface than those on the surface of TiO_2. Notably, the adsorption equilibrium constant K value from BiOCl (0.38 L/μg) is also much larger than that of TiO_2 (0.093 L/μg), suggesting the adsorption of TCA on BiOCl is much stronger than that on TiO_2. The superior adsorption property of BiOCl could be a reason for their high photocatalytic activities.

The photocatalytic behaviors of the photocatalyst are highly dependent on its intrinsic properties, which are further determined by such as the particle size, morphology, defects and aggregation. BiOCl has a layered structure, consisting of $[Bi_2O_2]^{2+}$ layers sandwiched between two slabs of Cl^-. In the present study, to ensure the representativeness, the used BiOCl photocatalyst was sheet-like shape with exposed (001) facets, prepared by a typical hydrothermal method. It is proposed that the oxygen termination feature and the strain differences between interlayers and intralayers render the easy generation of surface oxygen vacancies (OVs), which are strong Lewis acids sites. The carboxylate group of TCA molecule can adsorb coordinatively on

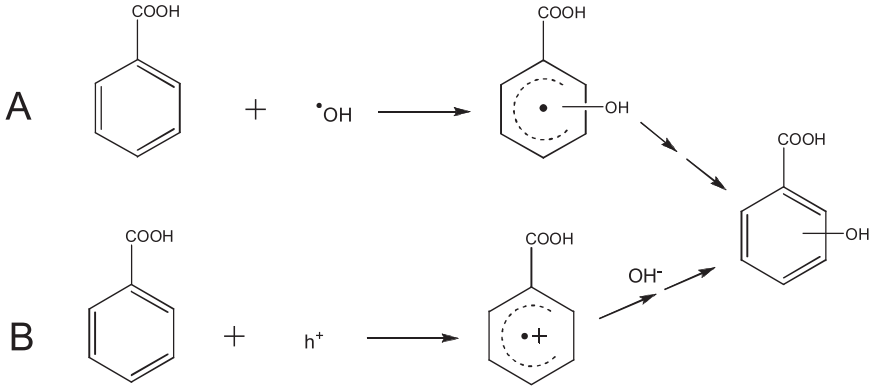

Scheme 1. Two pathways for the photocatalytic formation of hydroxylated benzoic acid.

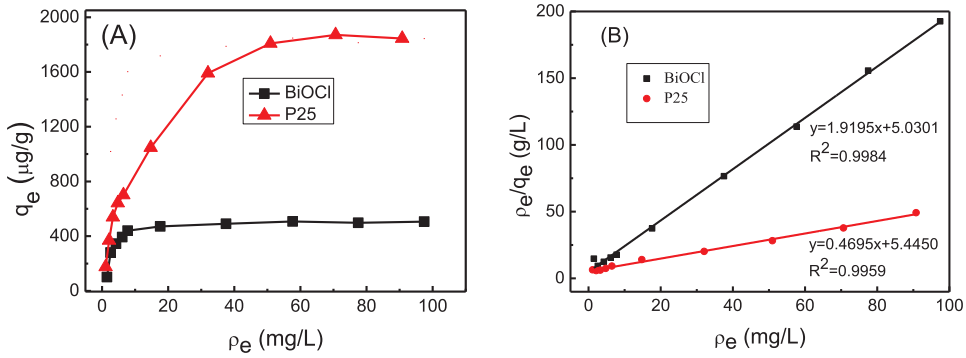

Fig. 4. (A) Adsorption isotherms of trichloroacetate on different photocatalysts at 298 K. (B) The isotherm fitted by Langmuir equation.

these OV sites in a bidentate or bridging configuration, as proposed on the adsorption of PFOA on In_2O_3 [28]. Such a strong interaction is believed to be beneficial for the photoinduced hole to transfer to the TCA. The theoretical calculation indicated that the bottom of valence band of BiOCl is composed of Cl3p and O2p, although the contribution of Cl3p is somewhat larger [12], which means that O2p and Cl3p have the similar energy level in BiOCl, and the photoinduced hole should be delocalized among the interlayer Cl atoms and the O atoms in the $[Bi_2O_2]$ layer. Accordingly, it is proposed that, once the substrate molecule is adsorbed on oxygen vacancies in the $[Bi_2O_2]$ layer, the hole on the O atoms in the layer is facile to transfer to the target molecules. On the other hand, the density of the surface oxygen vacancies (OVs) on TiO_2 is expected to be less than that on the BiOCl, which should be reason for the low surface active adsorption sites and low interactions strength for the adsorption of TCA by TiO_2. The weak interaction between the TCA and TiO_2 is unfavorable for the direct oxidation of TCA by holes. However, it is well studied that the adsorption of water molecule on the surface of TiO_2 sites is relatively strong, which would favor the hole transfer to these adsorbed H_2O molecule.

In addition, by the systematic comparison, we can get new insight into the reaction mechanism on both TiO_2 and BiOCl. For example, in the photooxidation on TiO_2 nanoparticle, it is proposed that the oxidation of organics (e. g. methanol) with weak interaction on TiO_2 nanoparticle proceeds via indirect mechanism ($OH^{\cdot}$ radicals). By contrast, for strong-interacting substrates such as formic acid, direct hole transfer pathway dominates the oxidation reaction [47,48]. In our studies, by comparing with the BiOCl system, we showed that, even for the strongly-adsorbed carboxylates, the photooxidation is dominantly initiated by indirect hole transfer pathway, while the direct hole transfer pathway plays a minor role. For the case of BiOCl, there was reports that the hydroxyl radical (indirect hole transfer pathway) is the main oxidative species for the oxidation of rhodamine B, methyl orange and phenol in the BiOCl photocatalysis [3]. We showed the indirect hole transfer pathway is not important to the degradation of chloroacetic acids and benzoic acid.

5. Conclusions

In this study, the detailed comparison on photocatalytic activity of the BiOCl and TiO_2 for the oxidative degradation of PHCAs and •OH-sensitive organic pollutants reveals that BiOCl and TiO_2 exhibit distinct photocatalytic behavior for the decomposition of PHCAs and oxidation of water molecules. BiOCl is a very effective photocatalyst for the removal of the PHCAs, while it is unfavorable to activate water into $^{\cdot}OH$ radicals. By contrast, TiO_2 prefers to oxidize photocatalytically water molecules, but its ability to oxidize PHCAs by hole transfer is quite weak. Our analysis on the mechanism underlying on the different activity of BiOCl and TiO_2 shows that the surface charge plays a minor role in their different adsorption and degradation behavior on BiOCl and TiO_2, and only the higher potential cannot explain well the superior activity of BiOCl for oxidation of PHCAs. The different site distribution for hole trapping and the adsorption of the PHCAs and water molecules on the surface of the two photocatalysts should be responsible for the different photocatalytic behaviors, which is deserved to be investigated further. The findings in the present study are not only helpful to our understanding on the specific structure-activity relationship of different photocatalytst, but also provide promising methods for the removal of resistant PHCAs coexisting with other labile organic compounds, as shown by the efficient degradation of PFOA and TCA in the presence of acetic acid.

Acknowledgements

This Special Issue is dedicated to honor the retirement of Dr. John Kiwi at the Swiss Federal Institute of Technology (Lausanne), a key figure in the topic of photocatalytic materials for the degradation of contaminants of environmental concern. This work was financially supported by National Natural Science Foundation of China (Nos. 21777168, 21525729, 21590811 and 21521062), by the "Strategic Priority Research Program" of the Chinese Academy of Sciences (No. XDA09030200) and the “CAS Interdisciplinary Innovation Team Program”. The authors would like to thank the assistance from Professor Yaqi Cai (Research Center for Eco-Environmental Sciences, Chinese Academy of Sciences) in analyzing the concentration of PFOA and intermediates.

Appendix A. Supplementary data

Supplementary material related to this article can be found, in the online version, at doi:https://doi.org/10.1016/j.apcatb.2018.09.058.

References

[1] X. Chen, S.S. Mao, Chem. Rev. 107 (2007) 2891–2959.
[2] H. Kisch, Acc. Chem. Res. 50 (2017) 1002–1010.
[3] F. Chen, H. Liu, S. Bagwasi, X. Shen, J. Zhang, J. Photochem. Photobiol. A: Chem. 215 (2010) 76–80.
[4] M.A. Gondal, X.F. Chang, Z.H. Yamani, Chem. Eng. J. 165 (2010) 250–257.
[5] D.-H. Wang, G.-Q. Gao, Y.-W. Zhang, L.-S. Zhou, A.-W. Xu, W. Chen, Nanoscale 4 (2012) 7780–7785.
[6] L. Ye, L. Zan, L. Tian, T. Peng, J. Zhang, Chem. Commun. 47 (2011) 6951–6953.
[7] Z. Song, X. Dong, N. Wang, L. Zhu, Z. Luo, J. Fang, C. Xiong, Chem. Eng. J. 317 (2017) 925–934.
[8] X. Liu, J. Zhong, J. Li, S. Huang, W. Song, Appl. Phys. A Mater. Sci. Proc. 119 (2015) 1203–1208.
[9] J. Li, H. Li, G. Zhan, L. Zhang, Acc. Chem. Res. 50 (2017) 112–121.
[10] H. Li, J. Shang, H. Zhu, Z. Yang, Z. Ai, L. Zhang, ACS Catal. 6 (2016) 8276–8285.
[11] K.-L. Zhang, C.-M. Liu, F.-Q. Huang, C. Zheng, W.-D. Wang, Appl. Catal. B: Environ. 68 (2006) 125–129.
[12] A.M. Ganose, M. Cuff, K.T. Butler, A. Walsh, D.O. Scanlon, Chem. Mater. 28 (2016) 1980–1984.
[13] Z.-Y. Zhao, W.-W. Dai, Inorg. Chem. 53 (2014) 13001–13011.
[14] T. Jing, Y. Dai, X. Ma, W. Wei, B. Huang, Phys. Chem. Chem. Phys. 18 (2016) 7261–7268.
[15] J. Jiang, K. Zhao, X. Xiao, L. Zhang, J. Am. Chem. Soc. 134 (2012) 4473–4476.

[16] K. Zhao, L. Zhang, J. Wang, Q. Li, W. He, J.J. Yin, J. Am. Chem. Soc. 135 (2013) 15750–15753.
[17] P. Casal, B. González-Gaya, Y. Zhang, A.J.F. Reardon, J.W. Martin, B. Jiménez, J. Dachs, Environ. Sci. Technol. 51 (2017) 2766–2775.
[18] C.-Y. Liao, X.-Y. Li, B. Wu, S. Duan, G.-B. Jiang, Environ. Sci. Technol. 42 (2008) 5335–5341.
[19] A. Xue, Z.W. Yuan, Y. Sun, A.Y. Cao, H.Z. Zhao, Chemosphere 141 (2015) 120–126.
[20] X. Li, S. Chen, X. Quan, Y. Zhang, Environ. Sci. Technol. 45 (2011) 8498–8505.
[21] H. Lin, Y. Wang, J. Niu, Z. Yue, Q. Huang, Environ. Sci. Technol. 49 (2015) 10562–10569.
[22] Y. Liu, S. Chen, X. Quan, H. Yu, H. Zhao, Y. Zhang, Environ. Sci. Technol. 49 (2015) 13528–13533.
[23] R. Dillert, D. Bahnemann, H. Hidaka, Chemosphere 67 (2007) 785–792.
[24] S.C. Panchangam, A.Y. Lin, K.L. Shaik, C.F. Lin, Chemosphere 77 (2009) 242–248.
[25] M. Sansotera, F. Persico, C. Pirola, W. Navarrini, A. Di Michele, C.L. Bianchi, Appl. Catal. B: Environ. 148-149 (2014) 29–35.
[26] P. Zhang, Z. Li, Nanotechnology for Water Treatment 79 and Purification 22 (2014), pp. 79–110.
[27] B. Zhao, P. Zhang, Catal. Commun. 10 (2009) 1184–1187.
[28] X. Li, P. Zhang, L. Jin, T. Shao, Z. Li, J. Cao, Environ. Sci. Technol. 46 (2012) 5528–5534.
[29] T. Shao, P. Zhang, L. Jin, Z. Li, Appl. Catal. B: Environ. 142-143 (2013) 654–661.
[30] C. Wu, A. De Visscher, I.D. Gates, RSC Adv. 7 (2017) 35776–35785.
[31] C. Hansch, A. Leo, R.W. Taft, Chem. Rev. 91 (1991) 165–195.
[32] R.G. Pearson, J. Am. Chem. Soc. 108 (1986) 6109–6114.
[33] M. Jonsson, J. Lind, T. Reitberger, T.E. Eriksen, G. Merenyi, J. Phys. Chem. 97 (1993) 11278–11282.
[34] A. Wold, Chem. Mater. (1993) 280–283.
[35] X. Xiao, C. Liu, R. Hu, X. Zuo, J. Nan, L. Li, L. Wang, J. Mater. Chem. 22 (2012) 22840–22843.
[36] H. Hori, A. Yamamoto, E. Hayakawa, S. Taniyasu, N. Yamashita, S. Kutsuna, H. Kiatagawa, R. Arakawa, Environ. Sci. Technol. 39 (2005) 2383–2388.
[37] H. Hori, Y. Nagaoka, M. Murayama, S. Kutsuna, Environ. Sci. Technol. 42 (2008) 7438–7443.
[38] Y.C. Lee, S.L. Lo, P.T. Chiueh, Y.H. Liou, M.L. Chen, Water Res. 44 (2010) 886–892.
[39] Z. Zhang, J.J. Chen, X.J. Lyu, H. Yin, G.P. Sheng, Sci. Rep. 4 (2014) 7418.
[40] L. Jin, P. Zhang, Chem. Eng. J. 280 (2015) 241–247.
[41] M.H. Cao, B.B. Wang, H.S. Yu, L.L. Wang, S.H. Yuan, J. Chen, J. Hazard, Mater. 179 (2010) 1143–1146.
[42] S.M. Mitchell, M. Ahmad, A.L. Teel, R.J. Watts, Environ. Sci. Technol. Lett. 1 (2014) 117–121.
[43] B. Yang, C. Jiang, G. Yu, Q. Zhuo, S. Deng, J. Wu, H. Zhang, J. Hazard. Mater. 299 (2015) 417–424.
[44] H. Moriwaki, Y. Takagi, M. Tanaka, K. Tsuruho, K. Okitsu, Y. Maeda, Environ. Sci. Technol. 39 (2005) 3388–3392.
[45] J. Cheng, C.D. Vecitis, H. Park, B.T. Mader, M.R. Hoffmann, Environ. Sci. Technol. 42 (2008) 8057–8063.
[46] Y. Qian, X. Guo, Y. Zhang, Y. Peng, P. Sun, C.-H. Huang, J. Niu, X. Zhou, J.C. Crittenden, Environ. Sci. Technol. 50 (2016) 772–781.
[47] I. Mora-Seró, T.L. Villarreal, J. Bisquert, Á. Pitarch, R. Gómez, P. Salvador, J. Phys. Chem. B 109 (2005) 3371–3380.
[48] T.L. Villarreal, R. Gomez, M. Gonzalez, P. Salvador, J. Phys. Chem. B 108 (2004) 20278–20290.